

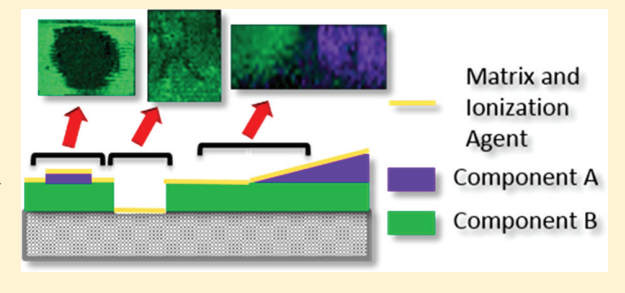
Surface Layer Matrix-Assisted Laser Desorption Ionization Mass Spectrometry Imaging: A Surface Imaging Technique for the Molecular-Level Analysis of Synthetic Material Surfaces

Kevin J. Endres, †, Jacob A. Hill, †, Loo Kuan Lu, Mark D. Foster, *, † and Chrys Wesdemiotis*, †, ‡

[†]Department of Polymer Science and [‡]Department of Chemistry, The University of Akron, Akron, Ohio 44325, United States

Supporting Information

ABSTRACT: Surface layer matrix-assisted laser desorption ionization mass spectrometry imaging (SL-MALDI-MSI) is a powerful new surface sensitive imaging technique to establish surface component localization of multicomponent polymer materials. This study demonstrates the ability of SL-MALDI-MSI to image defects from foreign materials, material absence, mechanical scribing, and solvent perturbation at the surface of low-molecular-weight poly(methyl methacrylate) and polystyrene thin films. The surface specificity of the SL-MALDI-MSI technique is validated by imaging polystyrene on poly(methyl



methacrylate) bilayer films; only polystyrene ions are detected from the surface of the unperturbed polystyrene layer. A key process enabling SL-MALDI-MSI is the solvent-free sublimation of matrix and salt uniformly on the sample's surface.

s the first point of contact with the environment, surfaces A sthe first point of contact with the partial state of materials in many applications. For example, they are particularly important in adhesion, coating durability, surface wetting, printing, membrane fouling, and protein adsorption and denaturation on biomaterials. Optimal performance in such applications may require consistent molecular (not just elemental) composition across the surface on length scales varying from nanometers to millimeters. This uniformity can be disrupted by various types of surface defects resulting from contaminants on the surface, damage from solvents, and alterations due to friction, abrasion, or light damage.1,2

Characterization of the surface composition and lateral uniformity of multicomponent synthetic polymer systems has faced two major challenges to be dealt with here. The first has been to characterize what is specifically at the surface (i.e., surface specificity or depth resolution). The second has been to provide adequate laterally resolved compositional information on the length scale needed. In recent decades, tremendous progress has been made regarding the first challenge, concerning surface specific compositional analysis. A few among the various techniques now available to provide surface compositional information include time-of-flight secondary ion mass spectrometry (ToF SIMS),^{3,4} other ion beam techniques,⁵ X-ray photoelectron spectroscopy (XPS),⁶ X-ray and neutron reflectivity (XR, NR),^{6–11} and plasmonics-based techniques such as surface enhanced Raman spectroscopy (SERS) and tip-enhanced Raman spectroscopy. 12 Each technique has advantages and disadvantages. Notably, none of these techniques is able to provide direct information on the actual composition of specific molecules at the surface, but rather, the techniques probe compositions of segments,

molecular fragments, or atoms; moreover, samples must often be labeled to generate an instrumental response.

Meeting the second challenge, obtaining laterally resolved information on surface composition, has been done in part with scanning options of a variety of techniques, including ToF SIMS, XPS, Auger spectroscopy, and tip-enhanced plasmonic techniques. 13-15 ToF SIMS imaging has been applied extensively to polymeric surfaces to investigate blend domains, ¹⁶ coatings, ¹⁷ hydrogels, ^{18,19} and nanoparticles. ²⁰ SIMS analyzes low-mass oligomers, fragments, and atomic ions. In contrast, matrix-assisted laser desorption ionization (MALDI) produces intact molecular ions, generating less convoluted spectra and making analysis simpler and more straightforward. The highest spatial resolution currently achievable with MALDI mass spectrometry imaging (MSI) is, however, only 1-5 μ m, 3,4 which is inferior to the 100 nm achievable by ToF SIMS-MSI. Also, without a chromophoric matrix (i.e., using laser desorption ionization, LDI), fragments formed by the laser can be imaged, but these species are not specific to the surface. The chromophoric character of dye molecules has been exploited to image organic and inorganic pigments in automotive coatings by LDI, via the detection of intact molecules or fragments thereof.21

Closely related to MALDI-MSI is surface-assisted laser desorption ionization (SALDI)-MSI, in which the sample is covered by sputtered platinum or silver nanoparticles that serve as the chromophoric matrix. ^{22,23} SALDI-MSI has been employed to image small molecules from inkjet ink on printed

Received: July 19, 2018 Accepted: October 22, 2018 Published: October 22, 2018

paper²² and the distribution of the antioxidant Irganox 1010 on polystyrene (PS) films.²³ Significant fragmentation was observed in these experiments, pointing out that SALDI is a relatively hard ionization method in comparison to MALDI.

The majority of MALDI-MSI studies has been performed on biological samples. MALDI, especially when interfaced with time-of-flight (ToF) mass analysis, is however a wellestablished technique for characterizing synthetic polymers and additives as well, 24-26 which is due to its ability to form singly charged ions over a virtually infinite molecular weight range. MSI is widely used to determine the localization of peptides, proteins, drugs, and metabolites within biological tissues. Analogous information on the spatial distribution of oligomers, (co)polymers, additives, and degradation products within synthetic materials is highly desirable. Unlike biological tissues, which are mechanically sliced prior to MSI, both depth resolution (i.e., surface sensitivity) as well as lateral resolution are critical for understanding surface segregation, defects, and degradation on synthetic material surfaces. Applications of MALDI-MSI to address these issues are scarce. MALDI-MSI has been used to image changes on PS films as they were UVirradiated, 27 demonstrate photolithographic structuring for printing, ²⁸ determine the chemical composition and physical characteristics of polysulfone and polyvinylpyrrolidone dialyzer membranes,²⁹ analyze lipid adsorption and degradation in polyethylene joint implants,³⁰ and confirm tocopherol acetate absorption inside laminate films.³¹ In all of these studies, solutions of the matrix and cationizing salt were deposited onto the solid sample by spin-casting or spraying. This process can cause extraction, influence dynamics within the bulk of the material, and change the surface composition. Such changes make MALDI-MSI unsuitable for probing material surfaces which may differ in composition from the bulk.

Solvent-free sample preparation, developed for polymer analysis, ^{32–36} can be applied to surface characterization to avoid perturbing the surface. Solvent-free matrix deposition has been used for MSI of biological samples to control the sizes of the matrix crystals and produce more uniform crystal layers, improving MSI results. ^{37–39} Biological specimens are not completely dried, however, and the samples are typically cross sections of regions within an organ or tissue. These characteristics lead to extraction of analyte from deeper regions of the sample. Thus, the method is not surface-specific.

Surface sensitivity can be achieved with surface layer (SL)-MALDI-MS, which has been shown to have a depth resolution of <2 nm for low-molecular-weight polystyrene (PS).40 This probing depth was established by showing that when a Langmuir monolayer of poly(methyl methacrylate) (PMMA) sits atop a spun-cast PS film only the PMMA is sampled. Corroborating evidence for this surface specificity was obtained by using other polymers for the spun-cast film and top monolayer; consistently, only the polymer on the surface was observed by SL-MALDI.⁴⁰ Fouquet et al. applied this method to depth profile a polymer bilayer film by alternating SL-MALDI-MS analysis with ion beam etching.⁴¹ More recently, we have used SL-MALDI-MS to show entropically driven enrichment of lower-molecular-weight polymer chains at the surfaces of PS and PMMA films, 42 as well as enthalpically driven depletion of entire polymer chains from the surface of PS blend films containing chains differing only in a single end group. 43 SL-MALDI-MS provides direct, selective, and sensitive information about intact molecules at the surface

in minutes to hours without expensive and perturbing labeling methods.

Most MALDI imaging sample preparation procedures employ solvent-based matrix application that perturbs the surface due to solvent penetration into the sample. This problem is bypassed in the SL-MALDI-MSI technique presented here using solvent-free matrix application. The simultaneous deposition of matrix and ionizing agent is also key. MALDI imaging experiments have primarily been performed on biological tissues, which promote ionization by protonation and do not require the addition of salts to facilitate ion formation. Such salts are, however, needed for the ionization of most classes of synthetic materials. Here we demonstrate the successful sublimation of MALDI matrices blended with cationization salts onto the surface of synthetic materials. We also document the utility of SL-MALDI-MSI as a surface-specific analytical technique that images surfaces based on intact molecular ion detection and with the depth resolution characteristic of SL-MALDI-MS (<2 nm).⁴⁰ These capabilities are illustrated by the acquisition of images of various types of surface defects on PS and PMMA films caused by surface contamination (modeled by stamping), masking, scratching, and solvation.

EXPERIMENTAL SECTION

Film Fabrication. PMMA (7 kDa) with the connectivity H-[CH₂C(CH₃)COOCH₃]_n-H was purchased from Polymer Source Incorporated. Analysis of this sample by MALDI-MS yielded a bulk number-average molecular weight (M_n) of 6850 \pm 50 Da. PS with the connectivity s-C₄H₉-[CH₂CH(C₆H₅)]_n-H, synthesized by living anionic polymerization at The University of Akron, was found to have a bulk M_n of 6030 \pm 130 Da. The corresponding polydispersities (PDIs) were 1.01 for the 6 kDa PS and 1.03 for the 7 kDa PMMA. Thin PS films were prepared by spin-casting from toluene solutions of 1–3 wt % at a rate of 2000 rpm to obtain smooth and laterally uniform films. Films were spun cast onto silicon wafers cleaned in piranha solution. Film thicknesses were determined with a spectroscopic ellipsometer (VASE, M-200 UV-visible-NIR [240–1700 nm], J. A. Woollam Co., Inc., Lincoln, NE, U.S.A.).

Defect Formation. Defects were created on the films by stamping, masking, scratching, and solvating. PMMA films were prepared by spin-casting 3 wt % solutions of 7 kDa PMMA onto silicon substrates. For PS stamps, the PS and spun cast film were heated to 195 \pm 5 °C and 75 \pm 5 °C, respectively, in clean watch glasses placed in separate sand baths. The transfer of PS onto PMMA was achieved using a polydimethylsiloxane stamp that had been leached for >1 h in toluene using Soxhlet extraction. This allowed transfer of pure molten material, while subsequent cooling caused vitrification of the stamped material. Defects were also created by masking a substrate before spin-casting a thin film of 7 kDa PMMA. Scotch tape was placed on a silicon wafer in two locations to ensure that the PMMA was deposited on the tape in those regions rather than the silicon surface. After spin coating, the tape was removed, ensuring no PMMA was present on the wafer in those locations. Another type of defect was created mechanically in PMMA films by either scratching a stacked "UA" (University of Akron logo) into the film with acetone washed stainless steel tweezers or, for a sharper image, by laser etching this logo and an image of the university's kangaroo mascot. Finally, defects by solvation were created using bilayer

films. First, a 3 wt % toluene solution of 7 kDa PMMA was spun cast onto a silicon wafer to form a 119.2 \pm 0.0 nm thick film (as determined by ellipsometry). Then a PS layer was deposited by spin-casting a 1.5 wt % solution of 6 kDa PS in cyclohexane to form a layer 88.5 ± 0.2 nm thick. For one bilayer film, the PS layer was washed off with ca. 1.6 mL of cyclohexane from a syringe, and the sample was dried with nitrogen gas; ellipsometry showed a thickness change from 207.7 ± 0.2 nm on the unwashed section to 114.6 ± 0.0 nm on the washed section. The washed region had a deep blue color, consistent with a ca. 100 nm thick PMMA film, whereas the unwashed region had a yellowish color, indicating a larger thickness. With another bilayer film, the wafer was dipped in a bath of cyclohexane four times and dried with nitrogen gas after each dip; this modified procedure led to a sharper lateral interface.

Matrix and Cationizing Agent Sublimation. Matrix and cationizing agent were applied by sublimation, which was performed using a sublimation apparatus attached to a coldwater spigot inside a fume hood. Heat was supplied by a silicon oil bath, heated with a hot plate equipped with a temperaturecontrolled feedback monitor. The sublimation apparatus was kept under vacuum using a roughing pump attached to a Schlenk line, with a vacuum trap cooled with liquid nitrogen. Matrix and cationizing agent blends were loaded into the sublimation apparatus. Samples were attached with permanent double-sided Scotch tape to the condenser portion of the apparatus with the film facing the bottom of the apparatus, where matrix and cationizing agent(s) were located. The loaded apparatus was closed, vacuum was applied, and the cold-water flow was turned on to allow condensation. Lastly, the bottom 6 mm of the apparatus was lowered into the oil bath, which was kept at 90 $^{\circ}\text{C}$. Sublimation was continued for 3-4 h. Heating was then paused and the apparatus was allowed to cool to near room temperature before vacuum was stopped and samples were removed. All sublimated components were applied simultaneously under the same conditions, typically producing deposited layers with thicknesses between 150 and 300 μ m. DHB (2,5-dihydroxybenzoic acid) and DCTB (trans-2-[3-(4-tert-butylphenyl)-2-methyl-2propenylidene malononitrile) were employed as matrices and NaTFA (sodium trifluoroacetate) and AgTFA (silver trifluoroacetate) as cationizing salts. Relative quantitation of the matrix and salt deposited on the surfaces was not investigated here, but both are assumed to be present in all raster spots since ionization occurred in every position by adduct formation with the salt cation.

MALDI-MSI Data Acquisition. MALDI-MSI was performed on a Bruker UltraFlex-III MALDI-ToF/ToF mass spectrometer (Bruker Daltonics, Billerica, MA) equipped with a Nd/YAG laser (λ = 355 nm; 100 Hz repetition rate). The laser energy was adjusted to avoid fragmentation of the polymer and minimize "bleed over" into adjacent raster spot regions. FlexImaging software version 2.1 (Bruker Daltonics) was used for spectral acquisition and evaluation. Prior to SL-MALDI-MSI, optical images were recorded with an Epson optical scanner. Imaging resolutions were chosen on the basis of the FlexImaging 2.1 User Manual Guidelines. Before each measurement, the instrument was calibrated with an external standard (polystyrene with $M_n = 6.1$ kDa, PDI = 1.05; Scientific Polymer Products, Ontario, NY). All spectra were measured in positive linear mode to maximize ion transmission and sensitivity. The m/z range 3500-8500 was scanned, and

500 shots were accumulated at each raster spot for a spectrum. Specifications for image acquisition for each region-of-interest (ROI) are listed in Table 1. Acquisition times were in the range of 10 h, depending on the ROI area and spatial resolution.

Table 1. Region-of-Interest (ROI) Specifications for SL-MALDI-MSI Images

ROI	ROI area (cm²)	number of raster positions	spatial resolution $(\mu \mathrm{m})$
PS stamp on PMMA (Figure 1)	0.543	2414	150
PS stamp on PMMA (Figure S2)	0.550	2446	150
tape defect (Figure 2)	0.179	448	200
tape defect (Figure S3)	0.432	1081	200
scratch/etch (Figure 3)	0.464	1159	200
bilayer dip (Figure 4)	0.173	432	200
bilayer dip (Figure S4)	0.244	611	200
bilayer rinse (Figure S6)	0.936	2339	200

Images of defects caused by scribing or laser-etching were also were acquired on a Bruker RapifleX MALDI-ToF/ToF mass spectrometer at spatial resolutions of 200 and 35 μ m. The higher repetition rate of the smartbeam 3D laser of the RapifleX (10 kHz) enabled image acquisition in <1 h with improved sensitivity.

MALDI-MSI Data Analysis and Interpretation. For analysis and interpretation of the acquired MALDI-MSI data, peaks associated with oligomers from each polymer component were selected, and a pseudocolor was assigned to each distribution (green for sodiated or silverated PMMA and purple for silverated PS). A \pm 5 m/z window was considered for each oligomer to cover the entire isotope cluster. Images were constructed by normalizing peak intensities to that of the base peak in the selected ROI. After visual examination of the SL-MALDI image overlaid with the optical image, spectra were extracted from regions lacking ion signal and from regions containing abundant ions (Figure S1). Additionally, spectra were extracted laterally across the bilayer interface at each raster spot along a single row (indicated by a red line in Figures 4 and S6). Changes in surface composition (see intensity profiles in Figures 4 and S6) were recorded by averaging the intensity of PMMA oligomers with n = 50-57repeat units and PS oligomers with n = 49-55 repeat units across four laterally adjacent spots. Peaks with intensities above a 5% threshold (relative to base peak) were considered to account for background noise.

■ RESULTS AND DISCUSSION

Foreign Material Defect Analysis. Image resolution, laser intensity, and experimental acquisition time were varied to optimize the quality and appearance of the images. The MALDI matrices used were DHB, which is a common matrix in imaging of biological samples, and DCTB, which efficiently desorbs synthetic polymers. A higher laser power was necessary for desorption and ion formation with DHB than with DCTB, and both matrices required higher laser power for SL-MALDI imaging in comparison to conventional MALDI analysis. The increased laser intensity resulted in "bleed over" into other raster positions upon data acquisition at resolutions <100 μ m. Image quality also depended on the uniformity and thickness

of matrix deposition. A feature unique to SL-MALDI imaging is that only material in contact with the matrix is desorbed intact; ⁴⁰ hence, signal is generated only from the top 2 nm of the surface, resulting in weak peak intensities (10–100 au/500 shots). An additional limitation on intensity is posed by the ionization efficiencies of the polymer components in a surface.

Polymer thin films were chosen to test SL-MALDI-MSI as a novel surface imaging technique, in continuation of our recent SL-MALDI-MS studies on segregation phenomena in thin films prepared from PS or PMMA blends. 42,43 For imaging PS stamps on PMMA, a layer of DHB matrix and NaTFA cationizing salt was sublimated onto the entire surface of the sample. DHB was initially tested as matrix because it had been previously sublimated for MALDI-MSI of biological tissues. Na⁺ was chosen for cationization because the high ionization efficiency of PMMA by Na⁺ adduction would allow to probe the section of the surface area remaining unperturbed and still having PMMA exposed. Indeed, the images (Figures 1 and S2)

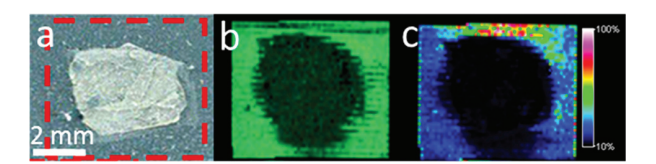
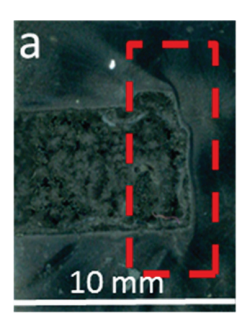


Figure 1. (a) Optical and (b,c) SL-MALDI images of a 6 kDa PS stamp defect on a 7 kDa PMMA thin film. The SL-MALDI images were constructed by summing the intensities of (b) [PMMA $_n$ + Na] $^+$ (n = 45-73) ions or (c) all ions within m/z 3500–8500. DHB and NaTFA (3:2 w/w) were sublimated onto the entire polymer—air interface. The PS stamped onto the surface hindered the ionization of PMMA underneath it. The SL-MALDI image clearly outlines the foreign material (PS), displaying defects specific to the surface. See Figure S2 for SL-MALDI-MSI of a different PS stamp.

clearly show the lack of ionization from the region where PS has been stamped onto the surface (Figure 1b) even when monitoring the entire m/z 3500–8500 range (Figure 1c) with a 5% low intensity threshold to eliminate background noise. The background noise does not contain any noticeable peaks resembling a PS or PMMA distribution (cf. Figure S1). The SL-MALDI images display $[PMMA_n + Na]^+$ ions which outline the PS stamps; each PMMA oligomer from n = 45-73 was selected and color labeled in green to reinforce the negative image displayed from the PS stamp defect (Figure 1b). Notably, there is absence of signal from the stamped area, which is attributed to the presence of PS on the surface in this region. The ion intensity differences observed in Figure 1c are attributed to topography effects on matrix/salt deposition resulting from the removal of PS melt in the upper region of the MS image. The SL-MALDI image of another PS stamp, applied to a different PMMA thin film, is shown in Figure S2 as evidence of the reproducibility of SL-MALDI-MSI for surface imaging at the molecular level.

Material Absence and Mechanical Scratching Defects. Additional film defects were investigated by adhering tape to different regions of a silicon wafer prior to spin-casting a 7 kDa PMMA thin film (Figures 2 and S3). The tape was removed prior to matrix/salt sublimation and imaging.

The red dashed boxes in Figures 2a and S3a indicate the ROIs analyzed. Sodiated PMMA_n oligomers with n = 50-72 were displayed in green to construct the corresponding SL-MALDI images (Figures 2b and S3b, respectively), which



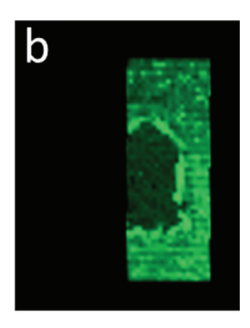


Figure 2. (a) Optical and (b) SL-MALDI images of a 7 kDa PMMA thin film in which some PMMA is missing because the tape masking that part of the wafer during spin-casting was removed. DCTB matrix and NaTFA (3:2 w/w) were sublimated onto the film—air interface after tape removal. The optical image shows the film after matrix/salt sublimation, with the region-of-interest indicated by the red dashed box. The SL-MALDI image was created by summing the intensities of $[PMMA_n + Na]^+$ (n = 50-72) ions and is displayed in green; it documents where PMMA is missing because it was removed when the tape was removed. See Figure S3 for the images of a PMMA film spun cast on a differently masked wafer.

clearly reveal the regions where the PMMA film was removed when the tape was removed. The higher signal intensities from regions adjacent to the edge of the tape (Figures 2b and S3b) are attributed to preferred PMMA deposition, during spincasting, at the change in surface height at the tape edge. Only noisy spectra like the one shown in Figure S1 were measured from within the taped region, corroborating the absence of PMMA from this area.

In a final set of tests, a visible mechanical defect was created after a thin film was cast by mechanical scratching of the University of Akron logo (U and A overlaid) or by laseretching the logo and mascot of the university's football team ("Akron Zips" and "Zippy", respectively). The scratch and etch were deep enough to penetrate the film and clear away most surface material (Figure 3).

DCTB matrix and NaTFA salt were sublimated as a test of providing an alternative matrix for desorption and imaging. DCTB has never before been sublimated for MALDI-MSI, but it is an excellent matrix for the ionization of polymers. DCTB vaporizes faster than DHB under the high-vacuum conditions of the MALDI source, which limits the acquisition time for imaging to 2–4 h. This shortcoming is compensated by the higher ionization efficiency, which produced good images for the ROI sizes and specified raster widths used (Table 1).

The defects caused by mechanical scratching or laser-etching of the film surfaces are clearly visible in the corresponding SL-MALDI images created by displaying in green the summed intensities of n-mers 50-72 (Figure 3). From closer examination of single spectra from the scratched films, it is evident that some regions within the scratches contained PMMA ions, while other scratched regions gave rise only to noise and were void of any PMMA distribution. This result is expected since material was not completely removed from the scribed area. Nevertheless, the "UA" scratch defect can be observed in the SL-MALDI images, most clearly when instrumentation with a 35 μ m spatial resolution is employed (Figure 3d). Contrast is sharper in the images of the laseretched features (Figure 3f) because laser etching removed material more efficiently from the PMMA film. In fact, details such as the tail of the kangaroo in the "Akron Zips" logo and the nose of the "Zippy" mascot are clearly discernible at 35 μ m

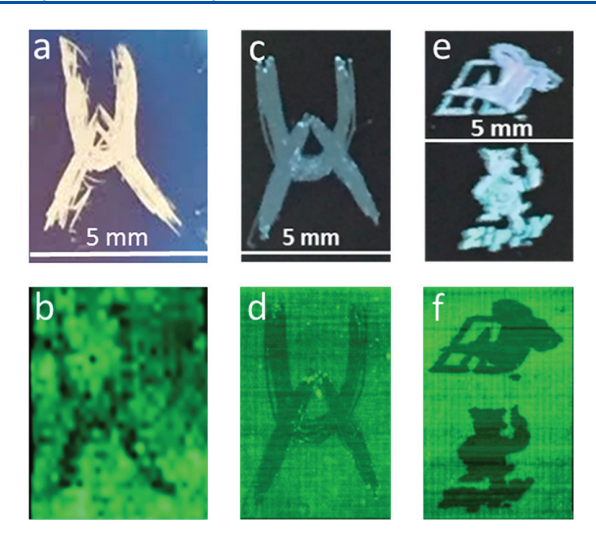


Figure 3. (a) Optical image of UA logo scribed on the surface of a 7 kDa PMMA film and (b) corresponding 200 μ m resolution SL-MALDI-MS image acquired with the UltraFlex mass spectrometer (see Experimental Section). (c) Optical image of UA logo scribed on the surface of a 7 kDa PMMA film and (d) corresponding 35 μ m resolution SL-MALDI-MS image acquired with the RapifleX mass spectrometer. (e) Optical images of "Akron Zips" logo (top) and "Zippy" mascot (bottom) laser-etched on the surface of a 7 kDa PMMA film and (f) corresponding SL-MALDI-MS images acquired with the RapifleX mass spectrometer. The optical images are shown before matrix and a sodium salt were sublimated onto the film. The SL-MALDI-MS images were constructed by summing the intensities of [PMMA $_B$ + Na]+ (n = 50–72) ions.

resolution. The use of a MALDI mass spectrometer with higher spatial resolution allowed for higher, more uniform signal as compared with the older Bruker equipment. While instrument selection was not the focus of this work, its consideration suggests improvements that can be made beyond our initial studies. Higher spatial resolution and increased sensitivity to enable higher spectral resolution (reflectron mode) are expected to result from ongoing testing and optimization of various matrix/salt sublimation conditions.

Solvent Perturbation Defects on the Top Layer of PS/PMMA Bilayer Films. In order to further demonstrate the surface specificity of SL-MALDI-MSI and its versatility in imaging defects on synthetic material surfaces, a model system was created by spin-casting a 6 kDa PS layer onto an underlying spun cast 7 kDa PMMA film. This bilayer film was dipped into cyclohexane solvent to dissolve and remove roughly half of the top PS layer, while leaving the PMMA bottom layer intact (Figure 4a). As a completely nonpolar solvent, cyclohexane selectively dissolves relatively nonpolar PS without affecting the underlying, much more polar PMMA.

For imaging this multicomponent film, we used a mixture of DCTB matrix with two cationizing salts, AgTFA and NaTFA, as Ag⁺ and Na⁺ are the cationizing species commonly used to ionize PS and PMMA, respectively. In the presence of the two salts, PMMA was found to ionize more efficiently by Ag⁺ adduction. This result, which is also observed upon conventional MALDI-MS analysis of a mixture of PS, PMMA, AgTFA, and NaTFA (cf. Figure S4), must be caused by the higher binding affinity of ester groups for Ag⁺ than for Na⁺. Consequently, [PMMA + Ag]⁺ ions, displayed in green, and [PS + Ag]⁺ ions, displayed in purple, were used for SL-MALDI-MSI of the partially washed PS/PMMA bilayer film.

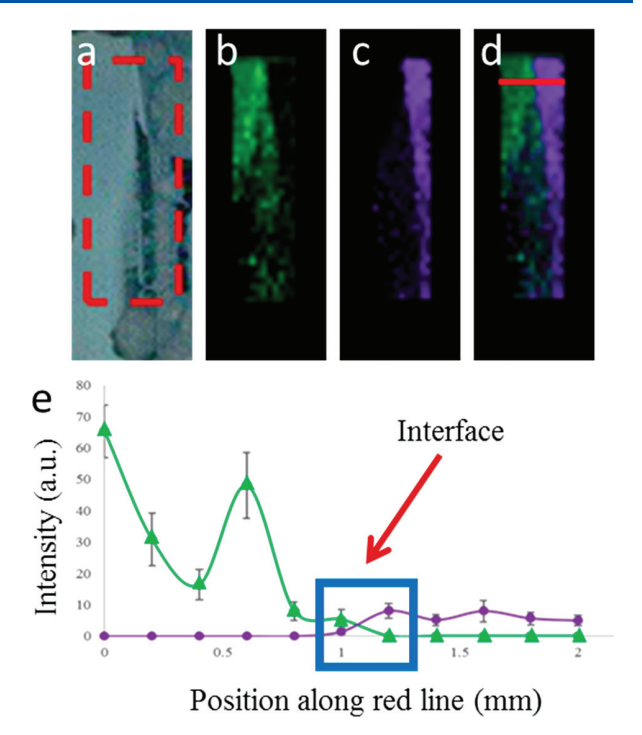


Figure 4. (a) Optical image and (b–d) SL-MALDI-MS images of a bilayer film prepared by spin-casting a 6 kDa PS layer onto a spun cast 7 kDa PMMA film, and then removing (from left side) half of the top PS layer by dissolving it in cyclohexane. The optical image is shown after a mixture of matrix and cationizing salts was sublimated onto the film. The area indicated by the red dashed line was imaged using summed $[PMMA_{50-57} + Ag]^+$ (green) or $[PS_{49-55} + Ag]^+$ (purple) intensities. (e) Intensity profile along the red line in (d) showing the uncovered PMMA from the washed region (left, in green) and the PS surface in the unperturbed part (right, in purple). See Figure S5 for the images from another bilayer film that was partially exposed to cyclohexane.

The SL-MALDI image (Figure 4b–d) gives intact molecular ion information on molecular weight and identity of each component at the surface. As expected, [PMMA + Ag]⁺ ions are detected only in the solvent perturbed region (green area in Figure 4b,d), whereas [PS + Ag]⁺ ions are observed only within the unperturbed region (purple area in Figure 4c,d). PMMA_n (n = 50-57) and PS_n (n = 49-55) oligomers were selected to display the SL-MALDI image, as this selection minimizes overlap between the two distributions (cf. Figure S4).

Additionally, an intensity profile was measured laterally across the material to quantitatively determine the composition at each raster position across the film (Figure 4e); it shows an immediate shift from PMMA to PS from one raster point to the adjacent point, unambiguously defining the interface between washed and unwashed surface. Ion signals diagnostic of each polymer are completely set apart to the respective region and no signal arising from PMMA is found in the unperturbed part of the surface, reinforcing the surface specificity of the imaging method. A replicate experiment, in which a vertically oriented bilayer film was partially dipped into cyclohexane solvent, further substantiated this specificity, as shown in Figure S5.

Using another bilayer film fabricated in the same fashion, roughly half of the top PS layer was removed by spraying cyclohexane rather than dipping. Nonetheless, again the

PMMA bottom layer was left undisturbed (Figure S6a). Because of the larger thickness of the film with the PS layer intact, that part of the sample appears yellowish in the optical image (Figure S6a). No color difference between the two parts of the sample film could be discerned after deposition of matrix and cationizing salts by sublimation (Figure S6b), which is due to the increase in thickness everywhere. The corresponding SL-MALDI-MS image shows that the interface between perturbed and unperturbed regions is not as sharp as when the film was dipped into cyclohexane (Figure S6c,d). Although $[PMMA_n + Ag]^+$ ions (green) dominate in the region perturbed by solvent (Figure S7) and $[PS_n + Ag]^+$ ions (purple) in the unperturbed region (Figure S8a), there are visible signals from $[PS_n + Ag]^+$ showing up in the region corresponding to the underlying PMMA, which probably is due to the rinsing not being quite complete. A noticeable compositional gradient is seen at the interface of these two sections of material as a result of insufficient rinsing (Figure S9) and less sharply defined rinsing front. This is evident in the intensity profile across the surface (Figure S6e), which shows a gradual switch in surface layer composition from PMMA (perturbed area) to a mixture (broad interface area) to PS (native area). It is important to note that no PMMA was observed at the surface of the unperturbed region (Figure S8b). Overall, the analysis of bilayer films (Figures 4 and S6) excellently demonstrates the ability of SL-MALDI-MSI to determine surface composition in different regions of a sample.

CONCLUSIONS

SL-MALDI-MSI is a novel surface imaging technique that capitalizes on the unique strengths of mass spectrometry, such as high sensitivity and specificity, to achieve conclusive chemical analysis of material surfaces. Using a uniform and solvent-free sample preparation protocol for the application of matrix and ionization agent, this technique consistently provides images of the material known to be on the surface. This is in keeping with earlier work showing that SL-MALDI probes molecules in the first 2 nm beneath the surface.

The utility of this technique has been demonstrated here for model samples fabricated under known conditions. It is expected that with better understanding of key factors in imaging and improvements in MALDI-related technology in general, the SL-MALDI-MS method can become a tool for studying more complex phenomena.

For the first time, a mixture of MALDI matrix (DCTB or DHB) and cationizing salt (AgTFA and NaTFA) was sublimated onto the surface of a multicomponent sample of synthetic polymers. With this approach, various surface features can be imaged. SL-MALDI-MSI is not limited to thin films and may be useful in a variety of applications where intact molecular information is desired. We are currently studying the procedures for sublimation of MALDI matrix and salt further in order to optimize them for laterally uniform deposition and best imaging sensitivity. This optimization is expected to facilitate applications to real-life samples in order to ascertain the mass ranges and types of macromolecules analyzable and extend the applicability of SL-MALDI-MS beyond the standard materials utilized in the present study. The data presented here establish SL-MALDI-MSI as the first analytical technique capable of providing surface images from intact molecular ions obtained exclusively from the sample within 2 nm of the surface.

ASSOCIATED CONTENT

S Supporting Information

The Supporting Information is available free of charge on the ACS Publications website at DOI: 10.1021/acs.analchem.8b03238.

Reference MALDI-MS spectrum of bulk PMMA, replicate SL-MALDI-MSI results, and single scans from different areas of SL-MALDI images (PDF)

AUTHOR INFORMATION

Corresponding Authors

*E-mail: wesdemiotis@uakron.edu. *E-mail: mdf1@uakron.edu.

ORCID 6

Jacob A. Hill: 0000-0001-7019-1779 Mark D. Foster: 0000-0002-9201-5183 Chrys Wesdemiotis: 0000-0002-7916-4782

Author Contributions

(K.J.E., J.A.H.) These authors contributed equally.

Notes

The authors declare no competing financial interest. Cleaning with the piranha solution (see Film Fabrication in the Experimental Section) was performed by following all precautions and considerations described in the Materials Safety Data Sheet.

ACKNOWLEDGMENTS

Support from the National Science Foundation (CHE-1808115 to C.W.) and the Defense Research Instrumentation Program (W911NF-10-1-067 to M.D.F.) is gratefully acknowledged. We thank Paul Kowalski, Shannon Cornett, Michael Easterling, and Bruker Daltonics for the 35- μ m SL-MALDI images measured on the RapifleX mass spectrometer.

REFERENCES

- (1) Mendoza-Navarro, L. E.; Diaz-Diaz, A.; Castañeda-Balderas, R.; Hunkeler, S.; Noret, R. *Int. J. Adhes. Adhes.* **2013**, *44*, 36–47.
- (2) Nimje, S. V.; Panigrahi, S. K. Int. J. Adhes. Adhes. 2015, 58, 70–79
- (3) Guenther, S.; Römpp, A.; Kummer, W.; Spengler, B. Int. J. Mass Spectrom. 2011, 305, 228-237.
- (4) Zavalin, A.; Todd, E. M.; Rawhouser, P. D.; Yang, J.; Norris, J. L.; Caprioli, R. M. *J. Mass Spectrom.* **2012**, *47*, 1473–1481.
- (5) Boerma, D. O. Nucl. Instrum. Methods Phys. Res., Sect. B **1990**, 50, 77–90.
- (6) Turner, N. H. Anal. Chem. 1988, 60, 377-387.
- (7) Russell, T. P. Mater. Sci. Rep. 1990, 5, 171-271.
- (8) Foster, M. D. Crit. Rev. Anal. Chem. 1993, 24, 179-241.
- (9) Elman, J. F.; Johs, B. D.; Long, T. E.; Koberstein, J. T. *Macromolecules* 1994, 27, 5341–5349.
- (10) Koberstein, J. T. J. Polym. Sci., Part B: Polym. Phys. 2004, 42, 2942–2956.
- (11) Gin, P.; Jiang, N.; Liang, C.; Taniguchi, T.; Akgun, B.; Satija, S. K.; Endoh, M. K.; Koga, T. *Phys. Rev. Lett.* **2012**, *109*, 265501.
- (12) Scherger, J. D.; Foster, M. D. Langmuir 2017, 33, 7818–7825.
 (13) Turner, N. H.; Schreifels, J. A. Anal. Chem. 2000, 72, 99–110.
- (14) Mahoney, C. M.; Weidner, S. M. In *Mass Spectrometry in Polymer Chemistry*; Barner-Kowollik, C., Gründling, T., Falkenhagen, J., Weidner, S., Eds.; Wiley-VCH: Weinheim, Germany, 2012; pp 149–207.
- (15) Xiao, L.; Schultz, Z. D. Anal. Chem. 2018, 90, 440-458.
- (16) Yunus, S.; Delcorte, A.; Poleunis, C.; Bertrand, P.; Bolognesi, A.; Botta, C. *Adv. Funct. Mater.* **2007**, *17*, 1079–1084.

(17) Brenda, M.; Döring, R.; Schernau, U. Prog. Org. Coat. 1999, 35, 183–189.

- (18) Sosnik, A.; Sodhi, R. N. S.; Brodersen, P. M.; Sefton, M. V. *Biomaterials* **2006**, *27*, 2340–2348.
- (19) Takahashi, H.; Emoto, K.; Dubey, M.; Castner, D. G.; Grainger, D. W. Adv. Funct. Mater. **2008**, *18*, 2079–2088.
- (20) Rafati, A.; Boussahel, A.; Shakesheff, K. M.; Shard, A. G.; Roberts, C. J.; Chen, X.; Scurr, D. J.; Rigby-Singleton, S.; Whiteside, P.; Alexander, M. R.; Davies, M. C. J. Controlled Release 2012, 162, 321–329.
- (21) Stachura, S.; Desiderio, V. J.; Allison, J. J. Forensic Sci. 2007, 52, 595–603.
- (22) Kawasaki, H.; Ozawa, T.; Hisatomi, T.; Arakawa, R. Rapid Commun. Mass Spectrom. 2012, 26, 1849–1858.
- (23) Satoh, T.; Niimi, H.; Kikuchi, N.; Fujii, M.; Seki, T.; Matsuo, J. *Int. J. Mass Spectrom.* **2016**, *404*, 1–7.
- (24) Montaudo, M. S.; Samperi, F.; Montaudo, M. S. Prog. Polym. Sci. 2006, 31, 277-357.
- (25) Gruendling, T.; Weidner, S.; Falkenhagen, J.; Barner-Kowollik, C. *Polym. Chem.* **2010**, *1*, 599–617.
- (26) Weidner, S.; Trimpin, S. Anal. Chem. 2010, 82, 4811–4829.
- (27) Crecelius, A. C.; Alexandrov, T.; Schubert, U. S. Rapid Commun. Mass Spectrom. 2011, 25, 2809–2814.
- (28) Crecelius, A. C.; Steinacker, R.; Meier, A.; Alexandrov, T.; Vitz, J.; Schubert, U. S. *Anal. Chem.* **2012**, *84*, 6921–6925.
- (29) Krueger, K.; Terne, C.; Werner, C.; Freudenberg, U.; Jankowski, V.; Zidek, W.; Jankowski, J. Anal. Chem. 2013, 85, 4998–5004.
- (30) Frohlich, S. M.; Archodoulaki, V.-M.; Allmaier, G.; Marchetti-Deschmann, M. Anal. Chem. 2014, 86, 9723–9732.
- (31) Tanaka, M.; Tanaka, E.; Obinata, N.; Matsui, T. Food Sci. Technol. Res. 2015, 21, 821–826.
- (32) Skelton, R.; Dubois, F.; Zenobi, K. Anal. Chem. 2000, 72, 1707–1710.
- (33) Przybilla, L.; Brand, J.-D.; Yoshimura, K.; Räder, H. J.; Müllen, K. Anal. Chem. **2000**, 72, 4591–4597.
- (34) Marie, A.; Fournier, F.; Tabet, J. C. Anal. Chem. 2000, 72, 5106-5114.
- (35) Trimpin, S.; Rouhanipour, A.; Az, R.; Räder, H. J.; Müllen, K. Rapid Commun. Mass Spectrom. 2001, 15, 1364–1373.
- (36) Trimpin, S.; Räder, H. J.; Müllen, K. Int. J. Mass Spectrom. 2006, 253, 13–21.
- (37) Hankin, J. A.; Barkley, R. M.; Murphy, R. C. J. Am. Soc. Mass Spectrom. 2007, 18, 1646-1652.
- (38) Puolitaival, S. M.; Burnum, K. E.; Cornett, D. S.; Caprioli, R. M. J. Am. Soc. Mass Spectrom. **2008**, 19, 882–886.
- (39) Trimpin, S.; Herath, T. N.; Inutan, E. D.; Wager-Miller, J.; Kowalski, P.; Claude, E.; Walker, J. M.; Mackie, K. *Anal. Chem.* **2010**, 82, 359–367.
- (40) Wang, S.; Li, X.; Agapov, R. L.; Wesdemiotis, C.; Foster, M. D. ACS Macro Lett. **2012**, 1, 1024–1027.
- (41) Fouquet, T.; Mertz, G.; Desbenoit, N.; Frache, G.; Ruch, D. *Mater. Lett.* **2014**, *128*, 23–26.
- (42) Hill, J. A.; Endres, K. J.; Mahmoudi, P.; Matsen, M. W.; Wesdemiotis, C.; Foster, M. D. ACS Macro Lett. 2018, 7, 487–492.
- (43) Hill, J. A.; Endres, K. J.; Meyerhofer, J.; He, Q.; Wesdemiotis, C.; Foster, M. D. ACS Macro Lett. **2018**, *7*, 795–800.
- (44) Asperger, A.; Niemeyer, D.; Henkel, C.; Hecht, S.; Cornett, S. Bruker RapifleX MALDI-ToF/ToF mass spectrometer; Bruker Daltonik GmbH: Bremen, Germany.
- (45) Owens, K. G.; Hanton, S. D. In MALDI Mass Spectrometry for Synthetic Polymer Analysis; Li, L., Ed.; John Wiley & Sons, Inc.: Hoboken, NJ, 2011; pp 129–158.
- (46) El Aribi, H.; Shoeib, T.; Ling, Y.; Rodriquez, C. F.; Hopkinson, A. C.; Siu, K. W. M. *J. Phys. Chem. A* **2002**, *106*, 2908–2914.